

1 **Major and minor elemental compositions of**
2 **streambed biofilms and its implications of riverine**
3 **biogeochemical cycles**

4
5 Short title: Biofilm geochemistry

6
7 Naoki Mori ^{1#}, Kenichiro Sugitani¹, Mariko Yamamoto¹, Rie Tomioka²,
8 Miyako Sato³, Naomi Harada³

9
10
11
12 ¹ Graduate School of Environmental Studies, Nagoya University, Nagoya 464-8601,
13 Japan

14 ² Graduate School of Bioagricultural Sciences, Nagoya University, Nagoya 464-8601,
15 Japan

16 ³Japan Agency for Marine-Earth Science and Technology, Yokosuka 237-0061,
17 Japan

18
19 # Present address: JCB Co. Ltd., Nagoya 460-0003, Japan

20 Corresponding author: Kenichiro Sugitani

21 Email: sugi@info.human.nagoya-u.ac.jp

22
23 *Key words:*

24 streambed biofilm, chemical compositions, dam reservoir, heavy metals

25

26

27 Abstract

28 Chemical compositions of streambed biofilms from a major river of central Japan (the
29 Kushida River) were obtained, with data of associated sediments (fine-grained
30 fractions < 63 μm) and dissolved components of waters, in order to provide
31 preliminary information about biogeochemical significance of streambed biofilms.
32 During the sampling period (July 31st to August 3rd, 2013), dissolved components of
33 the river waters were influenced by the dam reservoir. Concentrations of NO_3^- , silica
34 (as Si), SO_4^{2-} , PO_4^{3-} and Ca^{2+} decreased across the dam, whereas Fe and Mn
35 increased across the dam, and then decreased downstream rapidly. Streambed
36 biofilms contain significant amount of non-nutrient elements such as Al (up to 21% as
37 Al_2O_3 on water and others-free basis), indicating that they are contaminated as
38 siliciclastic (silt and clay) materials. Siliciclastic materials in the biofilms are basically
39 compositionally similar to fine-grained (< 63 μm) fractions of streambed sediments.
40 However, some elements such as Ca, P, Mn, and Zn are markedly enriched in the
41 biofilms. Particularly, Mn concentrations in the biofilm samples collected just below
42 the dam reservoir are very high (~4.0 wt %), probably due to accumulation from the
43 discharged water. Concentrations of trace elements such as P, Cr, Cu, Zn and V
44 appear to be controlled by amounts of Fe-oxides and/or Mn-oxides in biofilms.
45 Numbers of factors are involved in controlling chemical compositions of streambed
46 biofilms, including amount of contaminated siliciclastics, authigenic mineral formation,
47 adsorption of dissolved materials and microbial metabolisms. As demonstrated by this
48 study, systematic analyses including major elements and comparison with associated
49 sediments and waters could reveal biogeochemistry of this complex system.

50 *Capsule:*

51 *Chemical compositions of streambed biofilms can be interpreted by contaminated silts*
52 *and clays, bioaccumulation and adsorption onto Fe- and Mn-oxides.*

53

54

55 **1. Introduction**

56

57 Streambed biofilms composed mainly of microbes and extracellular polymeric
58 substances (EPS) are quite complex systems. They have been studied extensively in
59 the context of microbial community compositions, and primary production and nutrient
60 cycles of river ecosystem, and metal accumulation mechanisms (e.g, Battin et al.,
61 2003; Besemer et al., 2009; Dranguet et al., 2017; Drahota et al., 2014; Konhauser et
62 al., 1994; Tani et al., 2003). Biofilms can be regarded to represent consortia of
63 primary producers in river ecosystem, and are fed directly or indirectly as POM
64 (Particulate Organic Matter) by aquatic organisms such as grazers and collectors.
65 Thus these primary consumers and those of higher trophic levels could be affected by
66 chemistry of biofilms (e.g., Ancion et al., 2013; Farag et al., 2007; Rhea et al., 2006).
67 For example, Farag et al. (2007) demonstrated that metal concentrations in biofilms
68 and in aquatic invertebrates are closely related with each other. Also, Ancion et al.
69 (2013) reported that three trace metals (Zn, Cu & Pb) in biofilms explained the
70 community variations in bacteria and ciliate protozoa more than those in sediments.
71 Significance of inorganic geochemistry of streambed biofilms has been well
72 demonstrated by these studies and others (e.g., Haack and Warren, 2003; Kamjunke
73 et al., 2015). To our knowledge, however, these and other previous geochemical
74 studies of streambed biofilms did not provide dataset of major elements as Si, Al, Ti,
75 Fe, Mn, Mg, Ca, Na, K and P, despite concentrations of these elements provide basic
76 information about what components contribute to biofilm chemical compositions and
77 are expected to give insights into dynamics of trace metals in biofilms. Thus, the
78 purposes of this study are to present the first comprehensive dataset of major and
79 minor elemental compositions of streambed biofilms, providing basis on how biofilms
80 contribute to biogeochemical cycles in the stream ecosystem.

81

82 **2. Materials and Methods**

83

84 *2.1. Sampling area*

85 The Kushida River originates from the Mount Takami (alt. 1, 249m) at the border
86 between Mie Prefecture and Nara Prefecture in central Japan. It flows 87km into the
87 Ise Bay and its basin area is 436km² (Fig. 1). The basement of the northern part is
88 composed mainly of granitic rocks, whereas that of the southern part consists of
89 schists (Geological Survey of Japan, 2014). Population at the upper and the middle
90 reaches is 15, 000 persons and that at the lower reaches is 16, 000 persons. The
91 basin of the Kushida River is occupied largely with forests, paddy and tea fields, and
92 residential lands. Industries are also present but of small scale. The Kushia River
93 water during the sampling season can be assumed to be pristine and its trophic level
94 is very low, as demonstrated by low BOD concentration (<1mg/l) (Chubu Regional
95 Bureau, 2013a). The Kushida River has many tributaries, most of which, except for
96 the Hachisu River and the Sana River, are very small. The Hachisu River is located at
97 the uppermost reaches and has a large dam (the Hachisu Dam) with height of 78 m,
98 effective water depth of 41m, and effective storage capacity of 29,400,000m³ (Chubu
99 Regional Bureau, 2014). The residence time of water in the dam reservoir is
100 calculated to be 78 days, based on an average inflow rate (4.30 m³/S) in 2009 and the
101 effective storage capacity.

102

103 *2.2. Sampling and sample treatment*

104 The samplings were performed from July 31st to August 3rd, 2013. We collected 31
105 water samples including 6 samples from the Hachisu River and 5 reference samples
106 from drainages and small tributary, which were not used for this study (Fig. 1).
107 Although we intended to collect biofilms and sediments at the same localities for the

108 water samples, actual collected number of biofilms are 26, among which only 17
109 samples were enough in amount for analyses of major and minor elements. Sediment
110 samples used for chemical analyses of fine fractions ($< 63\mu\text{m}$) were collected mainly
111 from dips of exposed boulders in stream and shores of the river. We collected and
112 analyzed 21 sediment samples, among which 17 samples corresponding to biofilm
113 samples were used in this study.

114 Water samples were filtered on site ($< 0.45 \mu\text{m}$) and stored pre-cleaned
115 polyethylene bottles (100ml). For samples subjected to heavy metal analyses,
116 polyethylene bottles were pre-washed with HNO_3 and 0.5ml HNO_3 were added to the
117 samples immediately back to the laboratory. Streambed biofilms were removed from
118 gravels using a plastic brush and suspended in a plastic bowl to remove coarse
119 fractions. Suspended fractions were pipetted and transferred into plastic test tubes.
120 The tubes were manually centrifuged on-site, and supernatants were removed. This
121 procedure was repeated until sufficient quantities (approximately 7ml) of streambed
122 biofilms were collected, although as described earlier some samples were not enough
123 for chemical analyses. The biofilm samples were stored in an icebox and transported
124 to the laboratory, where we disentangled biofilm with distilled water and removed
125 aquatic insects and large detritus. The samples were subsequently dried at 110°C for
126 48 hours, and then grinded using an agate mill. Sediment samples were dried at room
127 temperature for several days and then at 110°C for 48 hours. After being dried, they
128 were sieved and fractions less than $63\mu\text{m}$ were retrieved for analyses.

129

130 2.3. Analyses

131 pH, DO and temperature were analyzed on-site using glass electrode pH analyzer
132 and fluorometric DO analyzer. Cations (Na^+ , K^+ , NH_4^+ , Ca^{2+} , Mg^{2+}) and anions (Cl^- ,
133 NO_3^- , SO_4^{2-}) were analyzed using ion chromatography. Dissolved metals (Fe, Mn),
134 silica (as Si), and phosphorous were analyzed by Inductively coupled plasma

135 atomic-emission spectroscopy (ICP-AES) (IRIS ICAP, Nippon Jarrell Ash). Streambed
136 biofilms and sediments (<63 μm) were combusted at 500°C and then mixed with
137 lithium tetraborate in the ratio of 1:7. This mixed powder was melted in a high
138 frequency muffle furnace at 1100 °C to be glass bead, which was subjected to X-ray
139 fluorescence spectroscopy (XRF)(Axios-N system, PANalytical). Ten major elements
140 (Si, Ti, Al, Fe, Mn, Mg, Ca, Na, K, P) and 7 minor elements (Ba, Cr, Cu Ni, V, Y, Zn)
141 were analyzed. For some samples whose amounts were not enough for XRF
142 analyses, sample powders were admixed with standard rock sample powder (JG1a)
143 and the data were recalculated to obtain chemical compositions of biofilms. Organic
144 elements (C, H, N) of dried samples of biofilms were analyzed using an elemental
145 analyzer (Frash 2000, Thermo Scientific). Isotopic compositions of C and N in biofilms
146 were analyzed using a mass spectrometer (EA-Mass Spectrometr, Thermo Scientific).
147 Original chemical data of streambed sediments and water are available upon request.

148

149 **3. Results and Discussion**

150

151 *3.1. Influence of the dam reservoir to water qualities*

152 Concentrations of NO_3^- , SO_4^{2-} , PO_4^{3-} , silica and Ca decrease to variously degree from
153 10 % to nearly 100% of the upstream levels across the Hachisu Dam reservoir,
154 whereas Cl^- and K^+ do not change (Fig. 2). Though not shown in this figure, Mg^{2+} and
155 Na^+ show a similar trend as K^+ . Concentrations of Fe and Mn increase drastically
156 through the dam reservoir, from less than 5ppb to nearly 40 ppb and more than 70
157 ppb, respectively (Fig. 2). While concentrations of the other components remain
158 nearly constant in the downstream from the dam, those of Fe and Mn exponentially
159 decrease. Inflow of such the Hachisu River water appears to influence some
160 component of the mainstream water. Concentrations of NO_3^- and silica of the
161 mainstream water are likely to be lowered by mixing of the Hachisu River water.

162 The above-described changes of dissolved components through the Hachisu
163 Dam reservoir may be explained by the results of previous studies (Beaulieu et al.,
164 2014; Hotta and Sugitani, 2007; Némery et al., 2016). Hotta and Sugitani (2007)
165 reported depletion of dissolved NO_3^- and SiO_2 in a small oligotrophic dam reservoir in
166 central Japan (Iwamura Dam, Gifu Prefecture) with much shorter retention time (ca.
167 10 days) of water than the Hachisu Dam (ca. 80 days); the dam surface and outflow
168 waters from ca. 8m depth show depletion of these nutrients relative to inflow waters
169 during summer. Hotta and Sugitani (2007) also demonstrated high concentrations of
170 dissolved Fe and Mn in the surface and outflow waters during the autumn and winter,
171 contrastive to their very low concentrations during summer and inflow waters.
172 Temperature data of water column of this dam indicate the development of thermal
173 stratification during summer and its disappearance in autumn. This thermal
174 stratification was in harmony with DO profile; the bottom water is anoxic during the
175 stratification. Thus, Hotta and Sugitani (2007) attributed high concentrations of Fe and
176 Mn of the surface and outflow waters of the Iwamura Dam in autumn to mixing of
177 surface and bottom waters caused by destruction of thermal stratification; the bottom
178 water has been enriched in Fe and Mn due to elution from the sediment under anoxic
179 condition.

180 In the present study, causes for decrease in NO_3^- and SiO_2 and increase in
181 Fe and Mn across the dam reservoir are less constrained, because the sample
182 collection was performed only in the summer. Also, the Hachisu Dam has three
183 different discharge gates, one of which is changeable with its height, making it difficult
184 to specify the depth from which outflow waters were discharged. Additionally,
185 retention of the discharged water in the shallow pool just below the dam, from which
186 the St. 3 sample was collected, possibly influenced the water quality, considering
187 luxuriance of green algae. Despite such ambiguities, we may suggest the possibility
188 that uptake by phytoplankton in the dam reservoir can be one of promising causes for

189 decrease in NO_3^- and SiO_2 , because other nutrients such as PO_4^{3-} , SO_4^{2-} and Ca^{2+}
190 also show decrease across the dam, while Cl^- and K^+ do not. As the sampling was
191 demonstrated from the end of July to August, the water stratification is assumed have
192 already been established in the dam reservoir. In fact, a minimum value of DO for the
193 bottom water recorded from 2003 to 2013 at the monitoring point is 4.8 mg/l, nearly
194 half of minimum values of middle and surface waters (9.5 and 9.0 mg/l, respectively)
195 (Chubu Regional Bureau, 2013b). Therefore denitrification should be considered as
196 another or additional cause for decrease in NO_3^- across the dam (e.g., Beaulieu et al.,
197 2014). As DO in the water sample collected from the shallow pool (St. 3) (6.19 ppm)
198 was higher than levels for anoxic or dysoxic conditions, it is difficult to attribute Fe and
199 Mn enrichment to in-situ reduction of Fe- and Mn-oxides. Enrichment in dissolved Fe
200 and Mn is therefore more likely explained by contribution of anoxic bottom water of the
201 dam reservoir where release of Fe and Mn from sediment occurred by abiogenic
202 reduction due to lowering of redox potential and related biological respiratory
203 reduction of Fe- and Mn-oxides (Beutel et al., 2008; Davison, 1993; Ito et al., 2008;
204 Munger et al., 2017).

205

206 *3.2. Geochemical characteristics of biofilms*

207 The streambed biofilms have various values of ignition loss from 18.1 % to 59.8 %
208 (Table 1). Concentrations of carbon and nitrogen known as bioessential elements also
209 range widely from 6.1 to 29.3 % and from 0.9 to 4.1 %, respectively. Significant
210 amounts of Al and Ti, which in general are not identified as bioessential (e.g., Maret,
211 2016), are also detected. Al and Ti concentrations range from 1.64 % to 7.32 % and
212 from 0.18 % to 0.5 %, respectively. Total Si concentrations range from 10.13 % to
213 17.87 %, showing a positive correlation with Al (c.c. = 0.61). Al and Ti in biofilms are
214 thought be contained exclusively in siliciclastic fractions (clays and silts), products of
215 weathering of basement rocks of tributaries, because these two elements are

216 basically stable during weathering and retained as solid phases (e.g., Young and
217 Nesbitt, 1998; Wei et al., 2003). This indicates that siliciclastic materials, in addition to
218 organic materials, comprise significant proportion of streambed biofilms. Silts and
219 clays suspended in river waters can be adsorbed by adhesive EPS (Extracellular
220 Polymeric Substances) of biofilms, particularly during the period of subsidence of
221 water level after flooding. On the other hand, the dominance of H, O, C, and N in
222 organic fractions of biofilms could obscure substantial features of geochemistry of
223 biofilms, because proportions of organic matter to siliciclastic material in biofilm are
224 various as indicated by data of ignition loss. Therefore, in order to examine precisely
225 geochemical features such as downstream trend and make comparison with
226 streambed sediments, the raw data of major elements are once recalculated to 100%
227 (water and others free basis) as oxide forms. Oxide-form concentrations of major
228 elements of the biofilms are basically similar to fine-grained sediments (< 63 μm) and
229 the Japanese Upper Crustal Composition representing averaged compositions of
230 surface rocks of Japanese Islands (Table 2). This may give impressions that inorganic
231 chemical compositions of streambed biofilms are controlled largely by clays and silts
232 settled down at each site. This is correct; however as inferred from e.g., unusually
233 high Mn concentration in biofilm (Table 1), more complex processes are involved in
234 geochemistry of biofilms.

235 Comparisons of Al-normalized values, often used to assess enrichment of
236 elements in sediments (e.g., Din, 1992), provide further insights into chemical
237 differences between biofilms and sediments at the same localities (Figs 3 and 4). The
238 distribution patterns indicate that Mg and K in the biofilms are derived largely from
239 contaminated silt and clay, whereas Ca and P, and to lesser extent Si appear to be
240 enriched in the biofilms, relative to the associated sediments. Fe, Mn, Cr, Cu, V and
241 Zn also show relative enrichment. Na and Co tend to be depleted in biofilms.
242 Enrichment or depletion of concentration of certain element in biofilm relative to

243 sediment could be interpreted in the context of bioaccumulation, microbial metabolic
244 reduction and resultant removal from biofilm, inorganic oxidation and reduction, and
245 adsorption on other phases such as Fe-oxide and organic matter (e.g., Carpentier et
246 al., 2003; Du Laing et al., 2009; Gounot, 1994; Weber et al., 2006). For example,
247 enrichment of Ca and P can be simply interpreted to reflect biomass in biofilms,
248 because they are representative bio-essential elements. Si-enrichment is also
249 attributed to populations of diatoms, which are the most dominant unicellular
250 eukaryotic organisms with silica frustule in the biofilm. As discussed later, enrichment
251 of the other elements could be interpreted adsorption on Fe- or Mn-bearing phases,
252 although detailed processes require further studies.

253 In biofilms from the Kushida River, carbon isotopic compositions ($\delta^{13}\text{C}$)
254 range significantly from -10.8 to -25.8 ‰, while nitrogen isotopic compositions ($\delta^{15}\text{N}$)
255 do from -0.4 to 5.3 ‰, respectively (Table 1). Nitrogen isotopic compositions show a
256 trend of becoming heavier downstream. This trend is consistent with the downstream
257 increasing trend of concentration of NO_3^- , Cl^- and PO_4^{3-} in river water (Fig. 2). As
258 populations of inhabitants increase downstream, these trends of dissolved
259 components in the river water are likely explained by influx of domestic wastewater.
260 Considering that domestic wastewaters enriched in organic matter generally have
261 high $\delta^{15}\text{N}$ (e.g., Wada, 2009; Sweeney et al., 1980), the downstream trend of $\delta^{15}\text{N}$ in
262 biofilm could be a consequence of assimilation of NO_3^- with relatively higher $\delta^{15}\text{N}$
263 values. Although denitrification, which could occur within biofilms and leave heavy
264 NO_3^- , may need to be considered as another or additional mechanism for the
265 N-isotopic trend (e.g., Cline and Kaplan, 1975; Maritotti et al., 1988), the clear
266 downstream trend favors the former interpretation.

267

268 3.3. Downstream trends of biofilm geochemistry

269 Downstream chemical trends of streambed biofilms could provide some constraints

270 on the cause of enrichment in Fe, Mn and other metals in the streambed biofilms
271 relative to sediments (Figs 3 and 4). As shown in Fig. 5, concentrations of these
272 elements in the streambed biofilms are markedly higher in the Hachisu River samples.
273 In particular, Mn concentrations of the Hachisu River samples range from 5.5 to 1.2%
274 (as water and others free basis), which are much higher than Japanese Upper Crustal
275 (JUC) value (0.085 % as Mn)(Togashi et al., 2000). Additionally, it rapidly decreases
276 downstream. A similar trend can be seen also for Fe, Ba, Co, and Zn. Although
277 dissolved metals in river waters we analyzed were only Mn and Fe, their trends shown
278 in Fig. 2 could give some constraints on mechanism responsible for their and others'
279 enrichments. Mn- and Fe-enrichment in the biofilms from the Hachisu River is best
280 explained by accumulation from the discharged water enriched in dissolved Mn and
281 Fe. Several pathways are potentially involved in this enrichment, including 1)
282 formation of fine metalliferous particles by oxidation of dissolved Fe and Mn and their
283 adhesion onto EPS of biofilms, 2) precipitation onto biofilm surface enriched in
284 functional groups, 3) precipitation as results of bacterial metabolisms (Fe- and
285 Mn-oxidizing bacteria), and 4) bioaccumulation (e.g., Carmichael et al., 2013; Clarke
286 et al., 1997; Gounot, 1994; Konhauser et al., 1994a; Weber et al., 2006). In either
287 case, like Fe and Mn, the other trace elements were probably enriched in the
288 discharged water and co-precipitated or adsorbed onto Fe- and Mn-oxides, which will
289 be discussed in the next section.

290

291 *3.4. Inter-element relationships in biofilms*

292 As mentioned above, mechanisms of enrichments of constituent elements of biofilms
293 are complex, but could be partially inferred from inter-element relationship.
294 Relationships of Al-normalized values of some selected elements to Fe/Al are shown
295 in Fig. 6, where biofilm and sediment samples from the Kushida and the Hachisu
296 rivers are discriminated.

297 Notably, P/Al, showing excess P relative to siliciclastic components,
298 positively correlates with the excess Fe (Fe/Al). Correlation coefficient between P/Al
299 and Fe/Al is 0.82, which is higher than those between P/Al and Ca/Al (0.6) and
300 between P and C (0.56). It is thus implied that significant fraction of the excess P in
301 the riverbed biofilms is bound to Fe-facies, probably Fe-oxides/hydroxides or
302 comprises ferric-phosphate (e.g., Fang et al., 2017; Konhauser et al., 1994b;
303 Ueshima et al., 2004). Some other elements such as Zn and V showing clear positive
304 correlations with Fe/Al are also considered to be associated with Fe- facies (e.g.,
305 Trivedi et al., 2001; Martinez and McBride, 1998; Wällstedt et al., 2010). On the other
306 hand, as can be seen from the relationship between Fe/Al and Mn/Al, the excess Mn
307 likely comprises a different facies such as Mn-oxides (Tani et al., 2003). Mn is
308 especially enriched in the biofilms collected from the lower reaches of the Hachisu
309 River. Although number of samples is limited, inter-elements relationships are
310 different from those of the Kushida River biofilms (Fig. 7). It is likely that Ba and Co
311 are incorporated into Mn-facies in the Hachisu lower reaches biofilms (e.g., Nicholson
312 and Eley, 1997; Gray and Malati, 1979).

313

314 **4. Conclusions**

315

316 A major river of central Japan (the Kushida River, Mie Prefecture) was studied for
317 chemical and isotopic (C and N) compositions of streambed biofilms, with waters and
318 riverbed sediments. Obtained results are as follows.

319 1) During the sampling period (July 31st to August 3rd, 2013), NO_3^- , silica, SO_4^{2-} , PO_4^{3-}
320 and Ca^{2+} concentrations markedly decreased across the dam constructed at the
321 major tributary, the Hachisu River. Discharged water from the reservoir was
322 characterized by high concentrations of Fe and Mn.

323 2) Streambed biofilms contain significant amount of inorganic components. Inorganic
324 components involved in the biofilms are derived largely from siliciclastic materials
325 (silt and clay) whose compositions are basically identical to those of fine-grained (<
326 63 μm) fractions of sediments.

327 3) However, some elements such as Si, Ca, P, Mn, Fe, Mn, Ba, Cr, Cu, V, and Zn are
328 enriched in the biofilms to various degrees on Al-normalization basis. Enrichment of
329 Fe and Mn in the biofilm samples collected just below the dam is attributed to
330 oxidation and accumulation of these elements (dissolved form) in the discharged
331 waters, and Fe- and/or Mn-oxides may have played a significant role for
332 accumulation of some elements.

333
334

335 **Declarations**

336 **Competing interests**

337 The authors declare that they have no competing interest.

338

339 **Authors' contributions**

340 KS proposed the topic, conceived and designed the study. NM carried out the
341 sampling and experimental studies conducted in Nagoya University, in collaboration
342 with MY and RT. MS and NH performed isotopic analyses, with NM.

343

344 **Acknowledgements**

345 We thank Dr. N. Ramamonjiso, Nagoya University for his support on sampling and Dr.
346 S. Ueno and Ms. Subuda, Nagoya University for his contribution to XRF analyses.
347 This work was supported by management expenses grants supplied by Nagoya
348 University to KS. This study was conducted as a part of Global Center of Excellence
349 Program: From Earth System to Basic and Clinical Environmental Studies. Professor
350 C. Takenaka and Associate professor K. Mimura, Nagoya University are also greatly

351 acknowledged for their kind permissions to our use of their facilities.

352

353 **References**

354

355 Ancion, P.-Y., Lear, G., Dopheide, A., Lewis, G.D., 2013. Metal concentrations in
356 stream biofilm and sediments and their potential to explain biofilm microbial
357 community structure. *Environmental Pollution* 173, 117-124.

358

359 Battin, T.J., Kaplan, L.A., Newbold, J.D., Hansen, M.E., 2003. Contributions of
360 microbial biofilms to ecosystem processes in stream mesocosms. *Nature* 426,
361 439-441.

362

363 Beaulieu, J.J., Smolenski, R.L., Nietch, C.T., Townsend-Small, A., Elovitz, M.S.,
364 Schubauer-Berigan, J.P., 2014. Denitrification alternates between a source and
365 sink of nitrous oxide in the hypolimnion of a thermally stratified reservoir.
366 *Limnology and Oceanography* 59, 495-506.

367

368 Besemer, K., Singer, G., Hödl, I., Battin, T.J., 2009. Bacterial community composition
369 of stream biofilms in spatially variable-flow environments. *Applied*
370 *Environmental Microbiology* 75, 7189-7159.

371

372 Beutel, M.W., Leonardo, T.M., Dent, S.R., Moore, B.C., 2008. Effects of aerobic and
373 anaerobic conditions on P, N., Fe, Mn, and Hg accumulation in waters overlying
374 profundal sediments of an oligo-mesotrophic lake. *Water Research* 42,
375 1953-1962.

376

377 Carmichael, M.J., Carmichael, S.K., Santelli, C.M., Strom, A., Bräuer, S.L., 2013.
378 Mn(II)-oxidizing bacteria are abundant and environmentally relevant members of
379 ferromanganese deposits in caves of the upper Tennessee River Basin.
380 *Geomicrobiology Journal* 30, 779-800.

381

382 Carpentier, W., Sandra, K., De Smet, I., Brigé, A., De Smet, L., Van Beeumen, J.,
383 2003. Microbial reduction and precipitation of vanadium by *Shewanella*
384 *oneidensis*. *Applied and Environmental Microbiology* 69, 3636-3639.

385

386 Chubu Regional Bureau (Ministry of Land, Infrastructure, Transport and Tourism,
387 2014. A summary of the Kushida River Basin System and tributaries (in
388 Japanese).
389 [http://www.mlit.go.jp/river/basic_info/jigyo_keikaku/gaiyou/seibi/pdf/kushida-4.p](http://www.mlit.go.jp/river/basic_info/jigyo_keikaku/gaiyou/seibi/pdf/kushida-4.pdf)
390 [df](http://www.mlit.go.jp/river/basic_info/jigyo_keikaku/gaiyou/seibi/pdf/kushida-4.pdf)
391

392 Chubu Regional Bureau (Ministry of Land, Infrastructure, Transport and Tourism),
393 2013a. Water qualities of Class A rivers in Chubu (in Japanese).
394 http://www.cbr.mlit.go.jp/kawatomizu/1kyukasen/pdf/h25_suishitsu_sankou.pdf
395

396 Chubu Regional Bureau (Ministry of Land, Infrastructure, Transport and Tourism),
397 2013b. A summary of the Hachisu Dam periodical report (in Japanese).
398 http://www.cbr.mlit.go.jp/kawatomizu/dam_followup/pdf/h24_hachisu-teiki.pdf
399

400 Cline, J.D., Kaplan, I.R., 1975. Isotopic fractionation of dissolved nitrate during
401 denitrification in the eastern tropical north pacific ocean. *Marine Chemistry* 3,
402 271-299.
403

404 Clarke, W.A., Konhauser, K.O., Thomas, J.C., Bottrell, S.H., 1997. Ferric hydroxide
405 and ferric hydroxysulfate precipitation by bacteria in an acid mine drainage
406 lagoon. *FEMS Microbiology Reviews* 20, 351-361.
407

408 Davison, W., 1993. Iron and manganese in lakes. *Earth Science Reviews* 34,
409 119-163.
410

411 Din, Z.B., 1992. Use of aluminium to normalize heavy-metal data from estuarine and
412 coastal sediments of Straits of Melaka. *Marine Pollution Bulletin* 24, 484-491.
413

414 Drahota, P., Škaloud, P., Nováková, B., Mihaljevič, M., 2014. Comparison of Pb, Zn,
415 As, Cr, Mo and Sb adsorption onto natural surface coatings in a stream draining
416 natural As geochemical anomaly. *Bulletin of Environmental Contamination and*
417 *Toxicology* 93, 311-315.
418

419 Dranguet, P., Le Faucher, S., Slaveykova, V.I., 2017. Mercury bioavailability,
420 transformations, and effects on freshwater. *Environmental Toxicology and*
421 *Chemistry* 36, 3194-3205.
422

- 423 Du Laing, G., Rinklebe, J., Vandecasteele, B., Meers, E., Tack, F.M.G., 2009. Trace
424 metal behavior in estuarine and riverine floodplain soils and sediments: A review.
425 Science of the Total Environment 407, 3972-3985.
426
- 427 Fang, H., Cui, Z., He, G., Huang, L., Chen, M., 2017. Phosphorous adsorption onto
428 clay minerals and iron oxide with consideration of heterogenous particle
429 morphology. Science of the Total Environment 605-606, 357-367.
430
- 431 Farag, A.M., Nimick, D.A., Kimball, B.A., Church, S.E., Harper, D.D., Brumbaugh,
432 W.G. (2007) Concentrations of metals in water, sediment, biofilm, benthic macro
433 invertebrates, and fish in the Boulder River watershed, Montana, and the role of
434 colloids in metal uptake. Archives of Environmental Contamination and
435 Toxicology 52, 397-409.
436
- 437 Geological Survey of Japan, 2014. Seamless Digital Geological Map of Japan
438 (1:200,000). <https://unit.aist.go.jp/igg/igi2-rg/seamless/seamlessE.html>
439
- 440 Gounot, A.-M., 1994. Microbial oxidation and reduction of manganese: consequence
441 in groundwater and applications. FEMS Microbiology Reviews 14, 339-349.
442
- 443 Gray, M.J., Malati, M.A., 1979. Adsorption from aqueous solution by δ -manganese
444 dioxide I. Adsorption and the alkaline-earth cations. Journal of Chemical
445 Technology and Biotechnology 29, 127-134.
446
- 447 Haack, E.A., Warren, L.A., 2003. Biofilm hydrous manganese oxyhydroxides and
448 metal dynamics in acid rock drainage. Environmental Science and Technology
449 37, 4138-4147,
450
- 451 Hotta, T., Sugitani, K., 2007. Dynamics of dissolved nutrients in a small oligotrophic to
452 mesotrophic dam –the case study for the Iwamura Dam, Gifu Prefecture,
453 Japan–. Chikyukagaku (Geochemistry) 41, 77-85.
454
- 455 Ito, A., Enta, K., Aizawa, J., Umita, T., 2008. Estimation of manganese source in a
456 dam reservoir and factors affecting manganese release from bottom sediments.
457 Journal of Japanese Society on Water Environment 31, 635-641.
458
- 459 Kamjunke, N., Mages, M., Buttner, O., Marcus, H., Weitere, M., 2015. Relationship

460 between the elemental composition of stream biofilms and water chemistry – a
461 catchment approach. *Environmental Monitoring and Assessment* 187, 432-445.
462

463 Konhauser, K.O., Schultze-Lam, S., Ferris, F.G., Fyfe, W.S., Longstaffe, F.L.
464 Beveridge, T.J., 1994. Mineral precipitation by epilithic biofilms in the Speed
465 River, Ontario, Canada. *Applied Environmental Microbiology* 60, 549-553.
466

467 Konhauser, K.O., Fyfe, W.S., Schultze-Lam, S., Ferris, F.G., Beveridge, T.J., 1994.
468 Iron phosphate precipitation by epilithic microbial biofilms in Arctic Canada.
469 *Canadian Journal of Earth Sciences* 31, 1320-1324.
470

471 Maret, W., 2016. The metals in the biological periodic systems of the elements:
472 concepts and conjecture. *International Journal of Molecular Sciences* 17,
473 66; <https://doi.org/10.3390/ijms17010066>
474

475 Mariotti, A., Landreau, A., Simon, B., 1988. ¹⁵N isotope biogeochemistry and natural
476 denitrification process in groundwater: Application to chalk aquifer of northern
477 France. *Geochemica et Cosmochimica Acta* 52, 1869-1878.
478

479 Martínez, C.E., McBride, M.B., 1998. Coprecipitation of Cd, Cu, Pb and Zn in iron
480 oxides: solid phase transformation and metal solubility after aging and thermal
481 treatment. *Clays and Clay Minerals* 46, 537-545.
482

483 Munger, Z.W., Shahady, T.D., Schreiber, M.E., 2017. Effects of reservoir stratification
484 and watershed hydrology on manganese and iron in a dam-regulated river.
485 *Hydrological Processes* 31, 1622-1635.
486

487 Némery, J., Gratiot, N., Doan, P.T.K., Duvert, C., Alvarado-Villanueva, R., 2016.
488 Carbon, nitrogen, phosphorous, and sediment sources and retention in a small
489 eutrophic tropical reservoir. *Aquatic Science* 78, 171-189.
490

491 Nicholson, K., Eley, M., 1997. *Geochemistry of manganese oxides: metal adsorption*
492 *in freshwater and marine environment*. Geological Society, London, Special
493 Publication 119, 309-326.
494

495 Rhea, D.T., Harper, D.D., Farag, A.M., Brumbaugh, W.G., 2006. Biomonitoring in the
496 Boulder River Watershed, Montana, USA: metal concentrations in biofilm and

497 macroinvertebrates, and relations with macroinvertebrate assemblage.
498 Environmental Monitoring and Assessment 115, 381-393.
499

500 Sweeney, R.E., Kalil, E.K., Kaplan, I.R., 1980. Characterisation of domestic and
501 industrial sewage in southern California coastal sediments using nitrogen,
502 carbon, sulphur and uranium tracers. Marine Environmental Research 3,
503 225-243.
504

505 Tani, Y., Miyata, N., Iwahori, K., Soma, M., Tokuda, S., Seyama, H., Theng, B.K.G.,
506 2003. Biogeochemistry of manganese oxide coatings on pebble surfaces in the
507 Kikukawa River System, Shizuoka, Japan. Applied Geochemistry 18,
508 1541-1554.
509

510 Togashi, S., Imai, N., Okuyama-Kusunose, Y., Tanaka, T., Okai, T., Koma, T., Murata,
511 Y., 2000. Young upper crustal chemical composition of orogenic Japan Arc.
512 Geochemistry, Geophysics, Geosystems 1, 1-45.
513

514 Trivedi, P., Axe, L., Tyson, T.A., 2001. An analysis of zinc sorption to amorphous
515 versus crystalline iron oxides using XAS. Journal of Colloid and Interface
516 Science 244, 230-238.
517

518 Ueshima, M., Fortin, D., Kalin, M., 2004. Development of iron-phosphate biofilms on
519 pyritic mine waste rock surfaces previously treated with natural phosphate rocks.
520 Geomicrobiology Journal 21, 313-323.
521

522 Wada, E., 2009. Stable $\delta^{15}\text{N}$ and $\delta^{15}\text{C}$ isotope ratios in aquatic ecosystems.
523 Proceedings of the Japan Academy, Series B, Physical and Biological Sciences
524 85, 98-107.
525

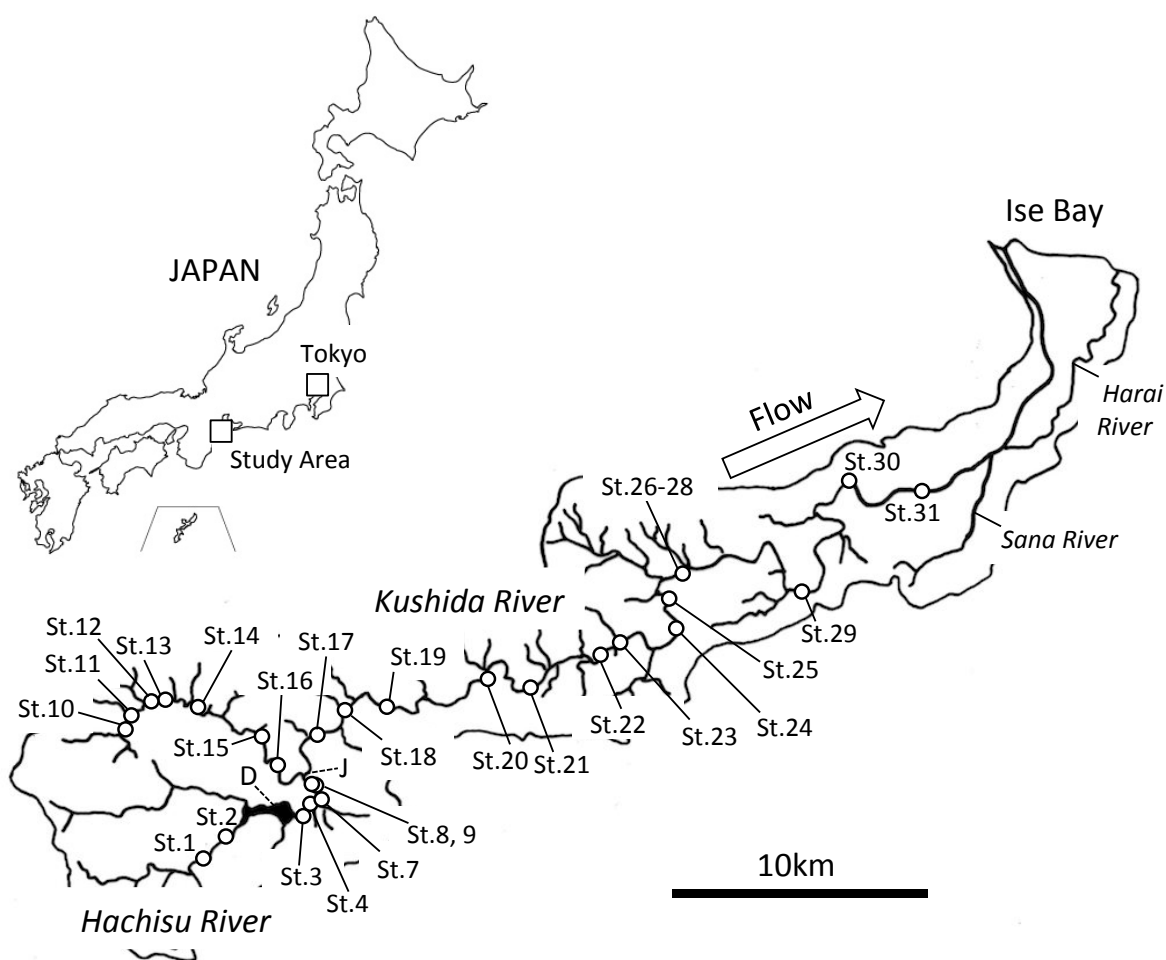
526 Wällstedt, T., Bjorkvald, L., Gustafsson, J.P., 2010. Increasing concentrations of
527 arsenic and vanadium in (southern) Swedish streams. Applied Geochemistry 25,
528 1162-1175.
529

530 Weber, K.A., Achenbach, L.A., Coates, J.D., 2006. Microorganisms pumping iron:
531 anaerobic microbial iron oxidation and reduction. Nature Reviews Microbiology
532 4, 752-764.
533

534 Wei, G., Liu, Y., Li, X., Shao, L., Liang, X., 2003. Climatic impact on Al, K, Sc and Ti in
535 marine sediments: evidence from ODP Site 1144, South China Sea.
536 *Geochemical Journal* 37, 593-602.

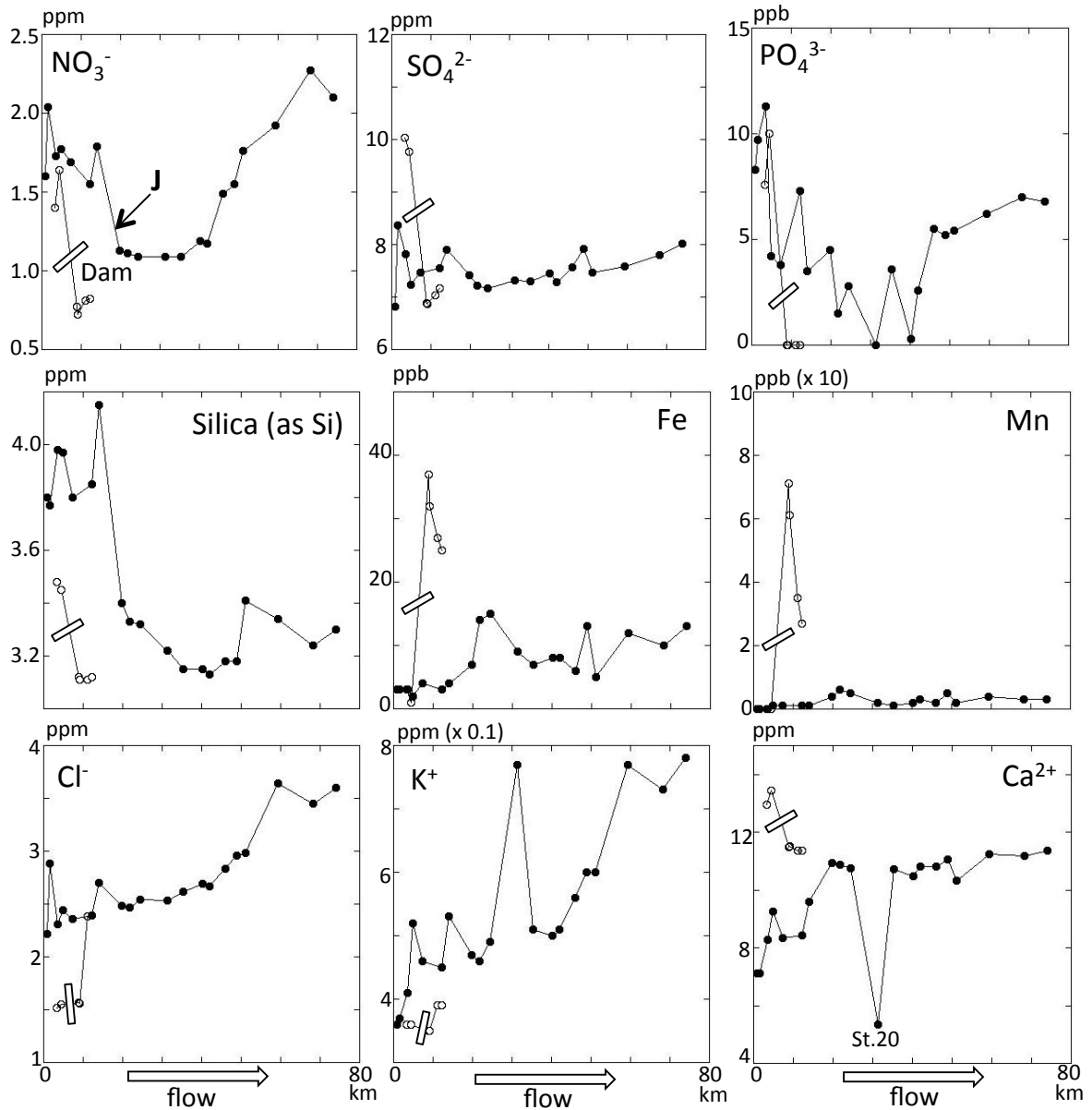
537
538 Young, G. and Nisbett, H.W., 1998. Processes controlling the distribution of Ti and Al
539 in weathering profiles, siliciclastic distribution of Ti and Al in weathering profiles,
540 siliciclastic sediment and sedimentary rocks. *Journal of Sedimentary Research*
541 68, 448-455.

542
543
544



545
546
547 Figure 1. Sampling Localities. D and J show the Hachisu dam and the junction,
548 respectively. Stations 5 & 6 are not shown, because these correspond to sampling
549 sites at the small tributary of Hachisu River and are not used in this work.

550



551

552

553 Figure 2. Downstream trends of NO_3^- , SO_4^{2-} , PO_4^{3-} , silica, Fe, Mn, Cl^- , K^+ , Ca^{2+} in
 554 water samples. Closed and open circles show the Kushida River samples and the
 555 Hachisu River ones, respectively. The junction of the Hachisu River and the Kushida
 556 River is representatively shown as J in the NO_3^- diagram.

557

558

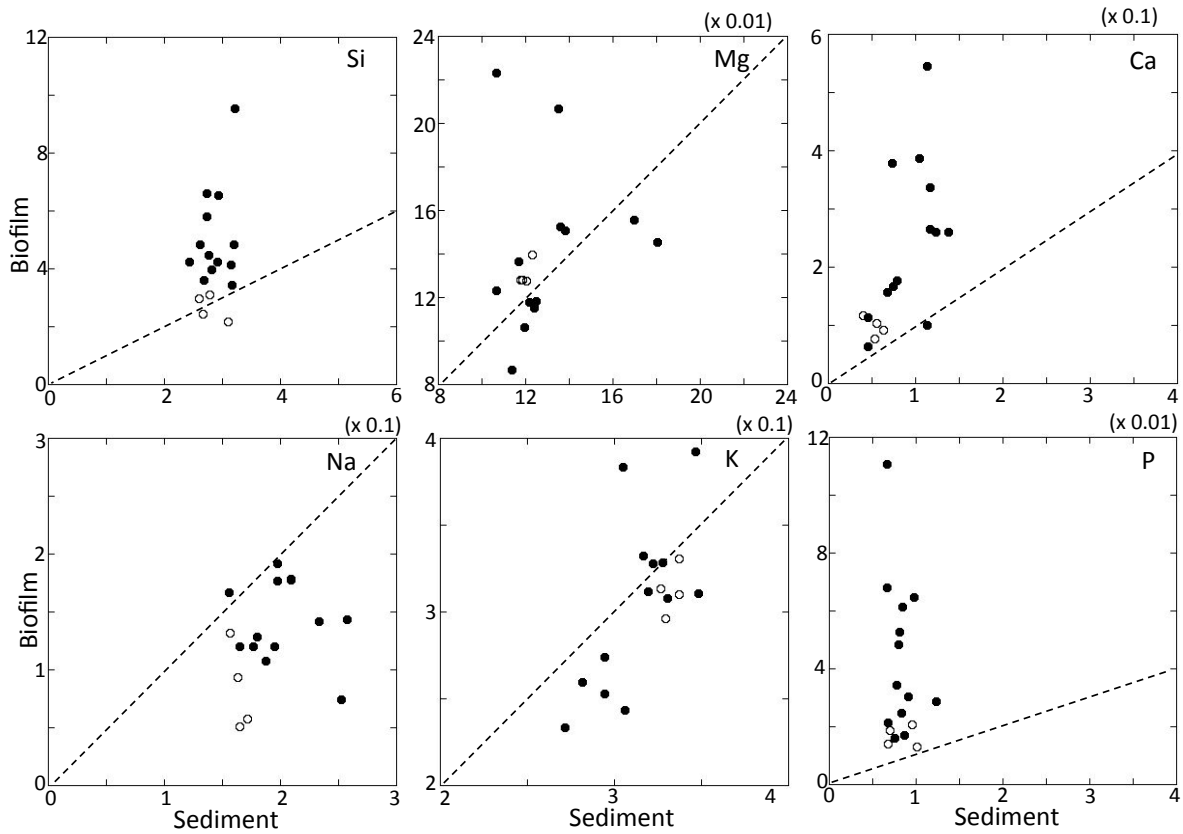
559

560

561

562

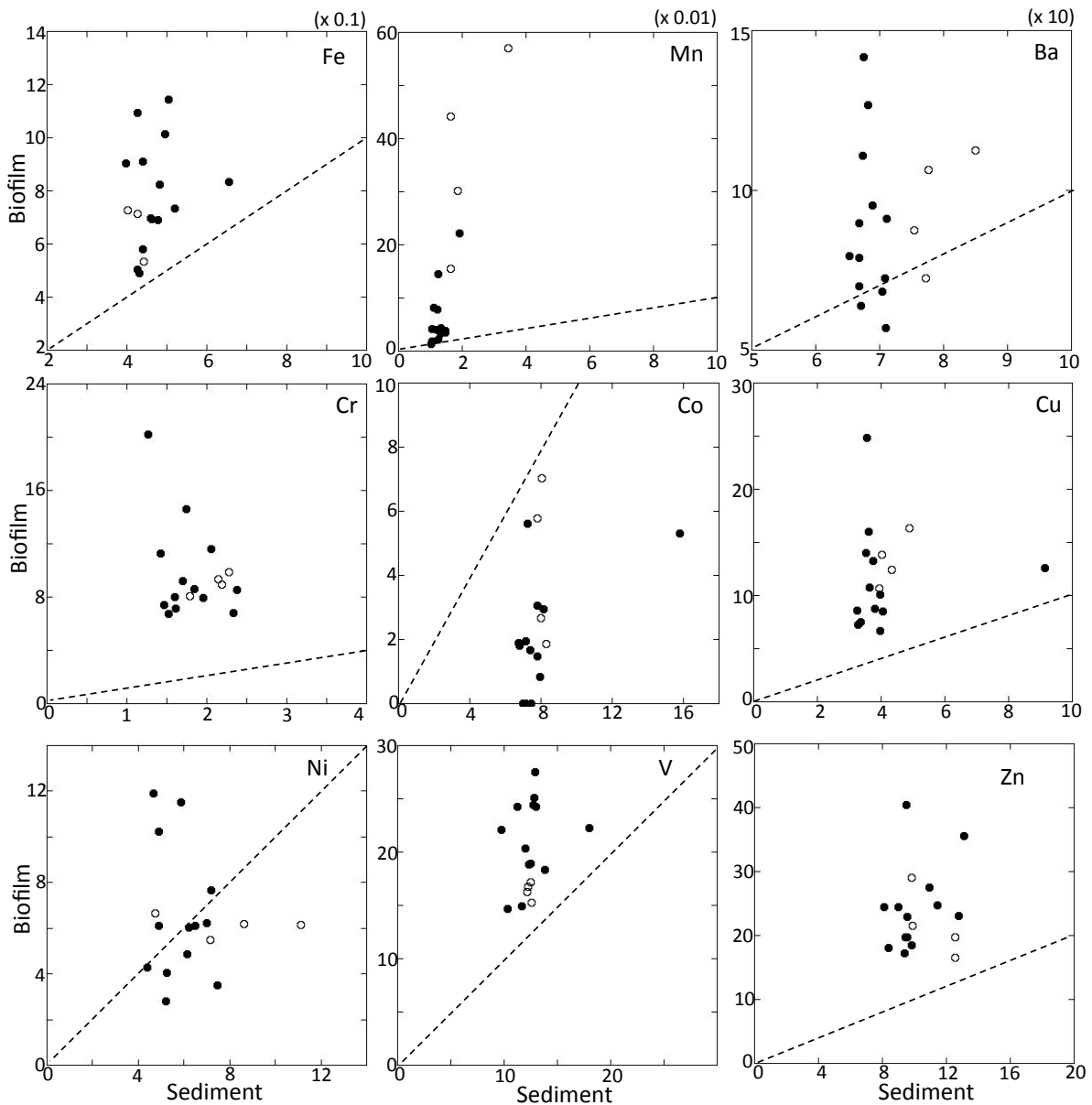
563
564
565



566
567
568
569
570
571
572
573
574
575
576
577
578
579
580
581
582

Figure 3. Relationships of Al-normalized values of elements (Si, Mg, Ca, Na, K, P) between biofilms and sediments. Plot on the dashed line indicates that at the sampling point biofilm and sediment have the same Al-normalized values. Closed and open circles show the Kushida River samples and the Hachisu River ones, respectively.

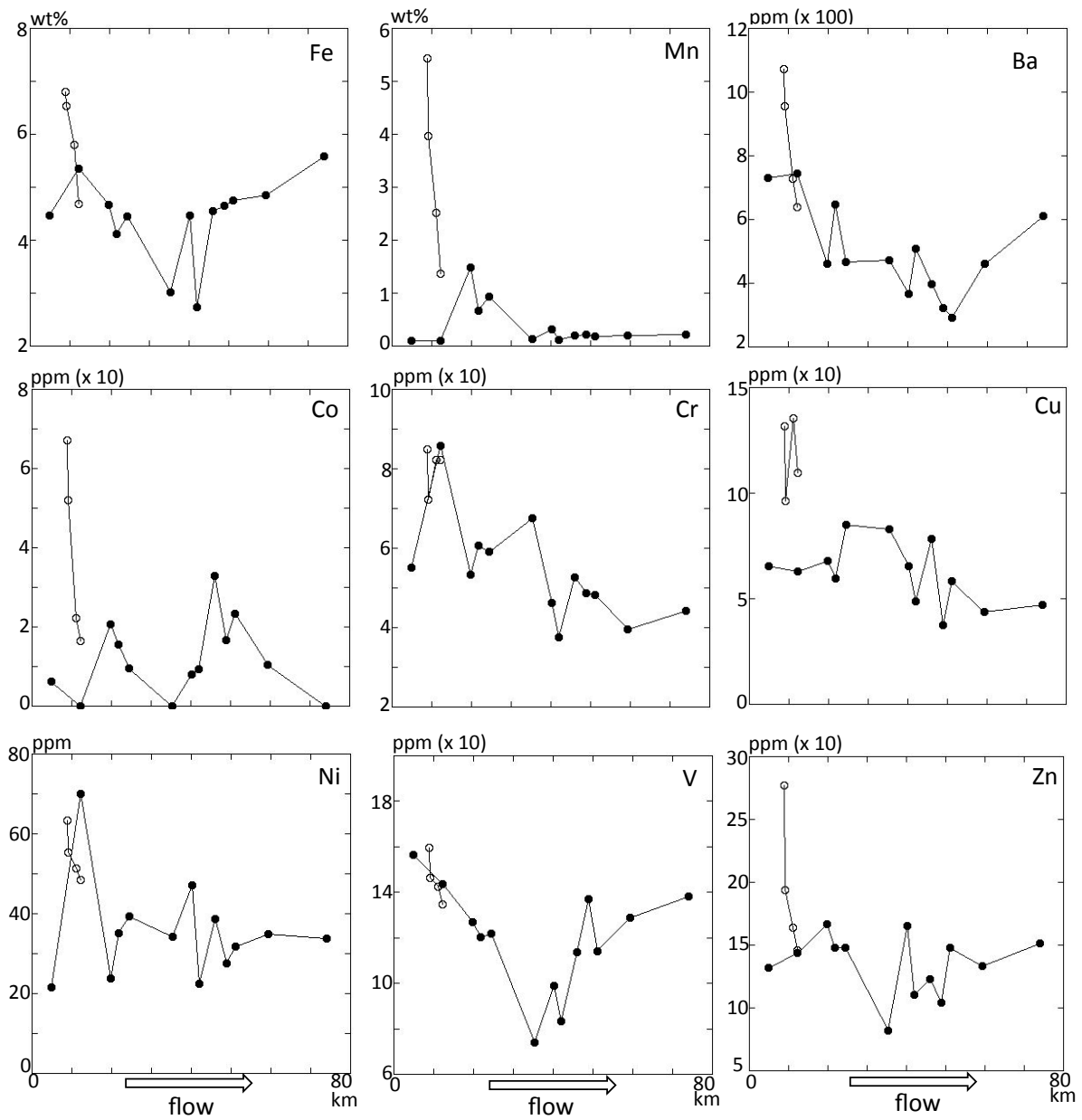
583
584
585



586
587
588
589
590
591
592
593
594

Figure 4. Relationships of Al-normalized values of elements (Fe, Mn, Ba, Cr, Co, Cu, Ni, V, Zn) between biofilms and sediments. Plot on the dashed line indicates that at the sampling point biofilm and sediment have the same Al-normalized values. Closed and open circles show the Kushida River samples and the Hachisu River ones, respectively.

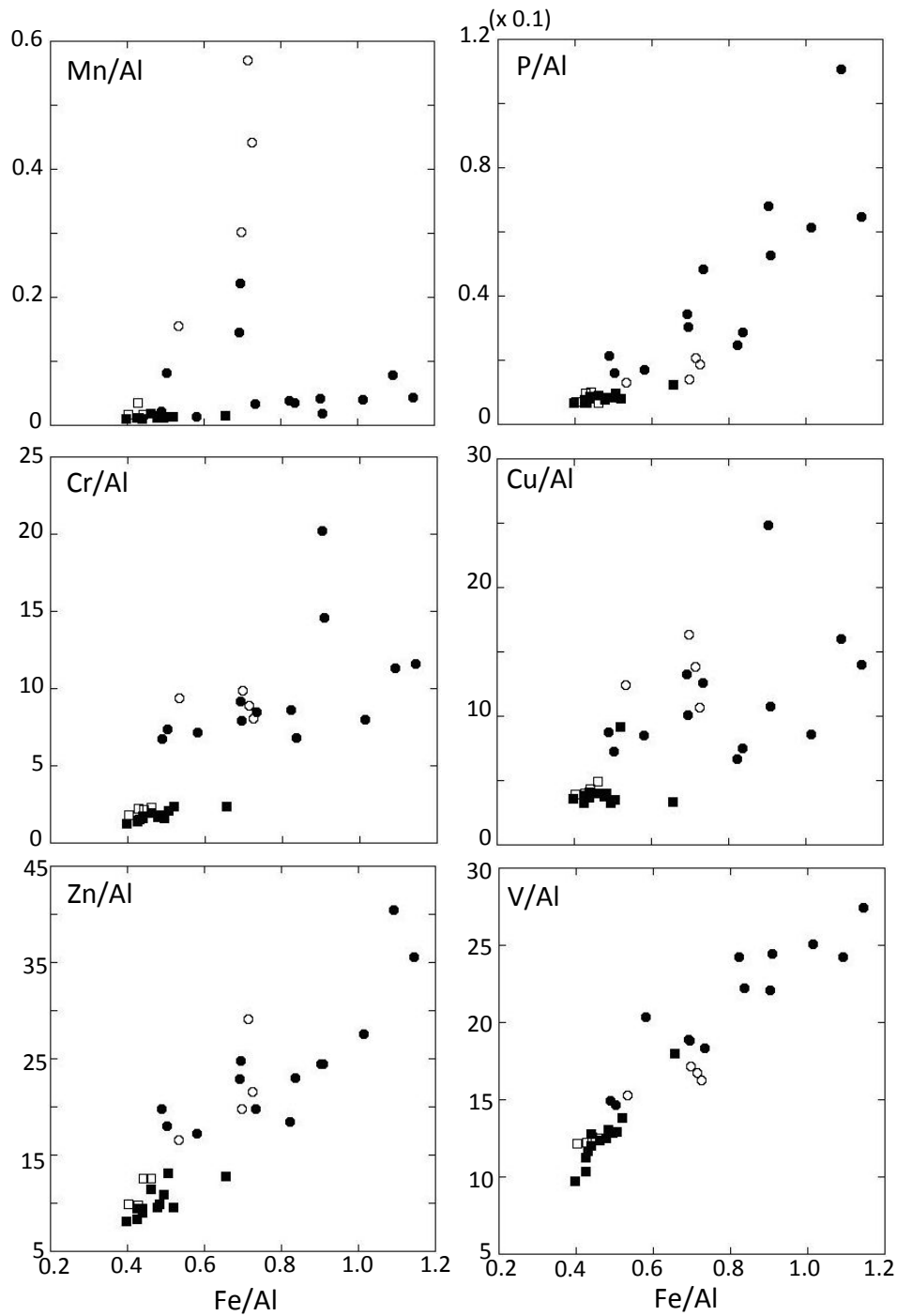
595
596
597



598
599
600
601
602
603
604
605

Figure 5. Downstream trends of Fe, Mn, Ba, Co, Cr, Cu, Ni, V and Zn (water- and others-free basis) in biofilm samples. Closed and open circles show the Kushida River samples and the Hachisu River ones, respectively.

606
607

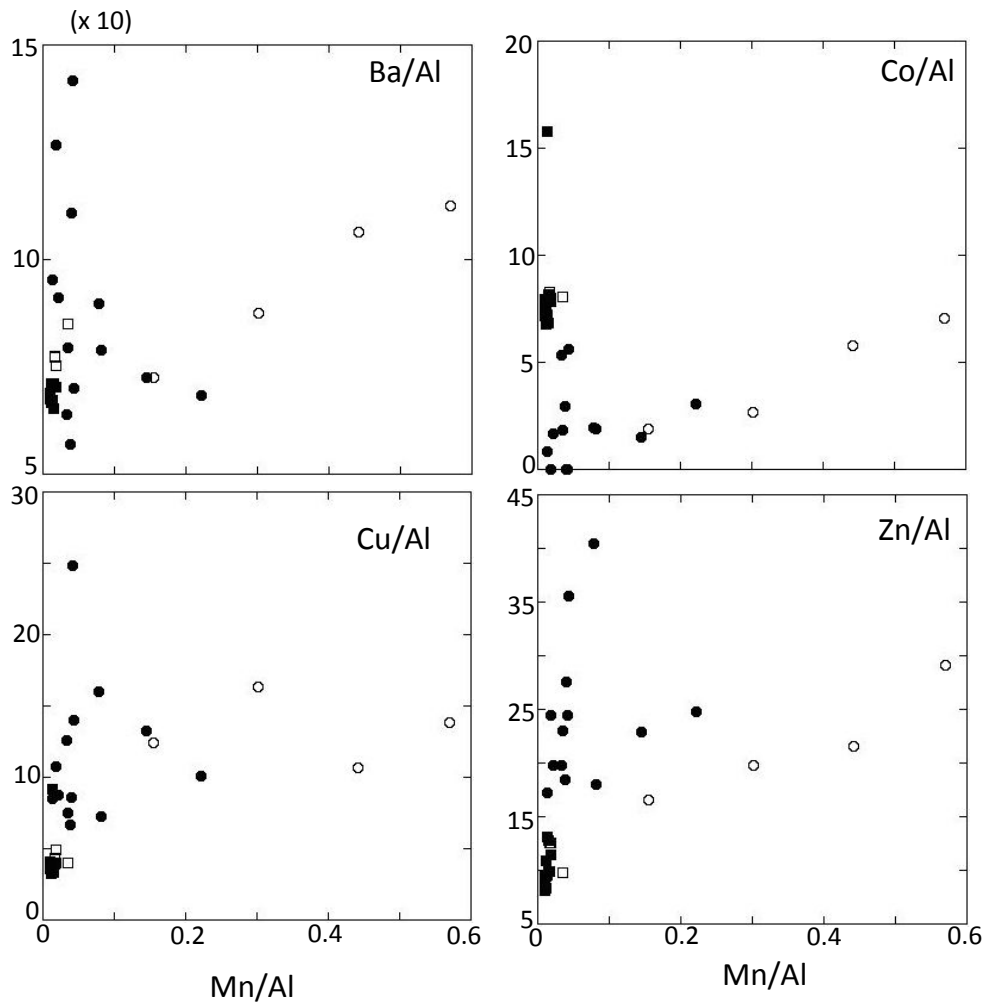


608
609
610
611
612

Figure 6. Relationship between Fe/Al and Al-normalized values of some elements (Mn, P, Cr, Cu, Zn, and V). Solid squares and open ones show the mainstream and the Hachisu River sediment samples, respectively. Solid circles and open one show the

613 Kushida mainstream and the Hachisu biofilm samples, respectively.

614



615

616

617 Figure 7. Relationship between Mn/Al and Al-normalized values of some selected

618 elements (Ba, Co, Cu, and Zn). Solid squares and open ones show the mainstream

619 and the Hachisu River sediment samples, respectively. Solid circles and open one

620 show the Kushida mainstream and the Hachisu biofilm samples, respectively.

621

622

623

624

625

626

Table 1 Chemical compositions of biofilms

Sample No.	3	4	8	9	13	15	17	18	19	21	22
Si (wt%)	15.66	14.43	19.41	22.43	15.63	20.07	19.81	22.97	17.98	17.13	10.74
Ti	0.455	0.409	0.417	0.45	0.48	0.343	0.358	0.414	0.33	0.176	0.214
Al	7.18	5.92	6.53	7.21	4.35	4.73	4.97	6.67	4.25	1.8	1.64
Fe	5.12	4.3	4.56	3.84	2.53	4.3	3.45	3.35	2.94	1.62	1.8
Mn	4.09	2.61	1.97	1.12	0.056	0.084	1.1	0.539	0.615	0.075	0.13
Mg	0.917	0.757	0.835	1.01	0.376	0.556	0.529	0.822	0.49	0.401	0.224
Ca	0.738	0.544	0.764	0.556	0.279	0.535	0.776	0.671	0.747	0.978	0.623
Na	0.411	0.301	0.607	0.95	0.769	0.786	0.637	0.945	0.508	0.258	0.122
K	2.25	1.95	2.02	2.13	1.45	1.45	1.55	2.07	1.39	0.705	0.631
P	0.149	0.11	0.092	0.094	0.074	0.249	0.15	0.107	0.146	0.122	0.182
Ig. Loss	24.7	34.2	21.4	18.1	43.4	19.6	26.2	18.8	34	46.2	59.8
N	1.4	1.8	2.3	0.9	0.9	3.0	1.9	1.6	2.3	2.9	4.1
C	11.4	15.9	16.8	8.3	6.1	23.5	13.8	10.0	16.8	22.5	29.3
$\delta^{15}\text{N}$ (‰)	1.7	0.9	1.2	1.3	0.5	-0.4	1.5	1.3	1.5	1.6	2.1
$\delta^{13}\text{C}$ (‰)	-25.8	-20.3	-21.0	-19.2	-17.8	-18.1	-17.4	-15.9	-15.4	-10.8	-13.3
Ba	807	629	571	523	414	598	340	526	308	254	147
Cr	63	47	64	67	31	68	39	49	39	36	18
Co	50	34	17	13	3	0	15	12	6	0	3
Cu	99	63	106	89	37	50	50	48	56	44	26
Ni	47	36	40	39	12	56	17	28	25	18	18
V	120	96	111	110	88	115	93	97	80	39	39
Y	22	16	18	20	13	10	9.7	18	15	0.5	4.7
Zn	208	127	128	119	74	115	122	120	97	44	66
	23	24	25	26	29	31	average	stdev.	min.	max.	
Si (wt%)	21.53	14.16	15.1	13.25	17.49	10.69	16.97	3.75	10.69	22.97	
Ti	0.274	0.325	0.402	0.237	0.381	0.327	0.35	0.09	0.18	0.48	
Al	3.71	3.42	3.11	2.01	3.62	2.4	4.32	1.87	1.64	7.21	
Fe	1.81	2.51	2.56	2.29	3.02	2.43	3.08	1.04	1.62	5.12	
Mn	0.08	0.115	0.118	0.086	0.126	0.096	0.76	1.14	0.06	4.09	
Mg	0.438	0.497	0.643	0.302	0.564	0.366	0.57	0.23	0.22	1.01	
Ca	0.616	0.89	1.2	0.676	0.939	0.634	0.71	0.21	0.28	1.20	
Na	0.713	0.611	0.553	0.216	0.434	0.288	0.53	0.25	0.12	0.95	
K	1.22	0.863	0.758	0.521	0.845	0.656	1.32	0.6	0.52	2.25	
P	0.08	0.165	0.077	0.13	0.104	0.147	0.13	0.04	0.07	0.25	
Ig. Loss	33.5	44.8	44.9	51.7	37.6	56.5	36.2	13.4	18.1	59.8	
N	2.0	3.9	2.3	3.8	2.1	4.1	2.4	1.1	0.9	4.1	
C	15.8	22.9	20.6	25.9	17.9	27.2	17.9	6.7	6.1	29.3	
$\delta^{15}\text{N}$ (‰)	2.1	3.4	2.7	3.6	3.8	5.3	2.0	1.38	-0.4	5.3	
$\delta^{13}\text{C}$ (‰)	-11.8	-15.4	-12.1	-13.7	-13.4	-13.6	-16.1	3.9	-25.8	-10.8	
Ba	338	219	177	140	287	265	384.9	193.0	140	807	
Cr	24	29	26	23	24	19	39.2	17.5	18	169	
Co	6	18	9	11	6	0	11.9	13.0	0	50	
Cu	32	43	20	28	27	20	49.3	26.5	20	106	
Ni	14	21	15	15	21	14	25.6	13.2	12	84	
V	55	62	75	55	80	60	80.9	26.0	39	120	
Y	11	9.9	11	2.2	7.8	5.5	11.4	6.2	0.5	22	
Zn	73	67	57	71	83	65	96.2	39.8	44	208	

Note: Sample No. corresponds to the number of sampling locality.

627

628

629

630

631

632

633

634

635

636

637
638
639

Table 2 Comparison of major elements between sediments and biofilms (water and other free-basis)

	Riverbed Sediments (< 63 μm)			Biofilm			JUC
	average	min.	max.	average	min.	max.	
SiO ₂	62.25±1.83	58.30	65.28	66.50±6.59	50.31	79.34	67.53
TiO ₂	0.91±0.11	0.65	1.17	0.72±0.15	0.34	0.91	0.62
Al ₂ O ₃	19.67±1.14	17.82	21.67	14.88±3.49	7.35	20.37	14.67
Fe ₂ O ₃	6.86±0.85	5.39	9.75	8.21±1.72	4.42	11.30	5.39
MnO	0.196±0.069	0.129	0.434	1.32±2.08	0.145	7.93	0.11
MgO	2.17±0.29	1.68	2.93	1.70±0.43	0.96	2.28	2.53
CaO	1.09±0.43	0.59	2.00	1.78±0.81	0.69	3.58	3.9
Na ₂ O	2.65±0.31	2.23	3.44	1.38±0.46	0.52	2.08	2.72
K ₂ O	3.99±0.37	3.33	4.55	2.93±0.76	1.62	4.10	2.42
P ₂ O ₅	0.194±0.034	0.145	0.294	0.584±0.311	0.283	1.32	0.12

Note: JUC is Japanese Upper Continental Crustal values (Togashi et al., 2000)

640
641
642